JOURNAL OF GUIDANCE, CONTROL, AND DYNAMICS
Vol. 28, No. 4, July–August 2005

Optimal Guidance Laws with Terminal Impact Angle Constraint

Chang-Kyung Ryoo*
Korea Advanced Institute of Science and Technology, Daejeon 305-701, Republic of Korea
Hangju Cho†
Agency for Defense Development, Daejeon 305-600, Republic of Korea
and
Min-Jea Tahk‡
Korea Advanced Institute of Science and Technology, Daejeon 305-701, Republic of Korea

Optimal guidance laws providing the specified impact angle as well as zero terminal miss distance are generalized for arbitrary missile dynamics. The optimal guidance command is represented by a linear combination of the ramp and the step responses of the missile's lateral acceleration. Optimal guidance laws in the form of the state feedback for the lag-free and the first-order lag system are derived, and their characteristics are investigated. Practical time-to-go calculation methods, which are important for the implementation of the optimal guidance laws, are proposed to consider the path curvature. Nonlinear and adjoint simulations are performed to investigate the performance of the proposed laws.

I. Introduction

IMPACT angle control has been widely used to satisfy the flight-path angle constraint. For antiship or antitank missiles, the terminal impact angle is important for warhead effect. An unmanned aerial vehicle can also have flight-path constraints, depending on its mission. For ballistic missiles, vertical impact on the target can reduce the miss distance produced by navigation errors. Previous works on impact angle control can be classified into two categories: optimal guidance laws[1–6] and other methods.[7,8]

In the approach of optimal guidance, the terminal impact angle controller is given by the solution to the linear quadratic optimal control problem. Kim and Grider[1] have proposed an optimal impact angle control guidance law for the reentry vehicle in the vertical plane. A simple rendezvous problem has been solved by Bryson and Ho,[2] where they include the position and the velocity component perpendicular to the specified rendezvous course into the cost to be minimized. If the rendezvous course is chosen to be identical to the predetermined collision course, the optimal solution can be used for impact angle control. Ryoo and Cho[3] have investigated an optimal guidance law for constant speed missiles with constraints on the impact angle and control input. Ben-Asher and Yaesh[4] present optimal guidance laws with weights on terminal velocity that can be translated as weights on the impact angle. A time-optimal control problem with constrained maneuverability has been investigated by Song and Shin.[5] The command generated by this guidance law is a bang-off-bang type, and the optimal switching time is the main interest of their work. An optimal impact angle control law for varying velocity missiles against maneuvering targets has also been studied by Song et al.,[6] where the guidance law is combined in cascade with a target tracking filter to predict the intercept point.

The methods of the second category are mainly concerned with additional bias terms of conventional proportional navigation guidance (PNG) required to control the impact angle. Kim et al.[7] have considered a time-varying bias, which is intuitively chosen as a combination of the state variables such as the line-of-sight (LOS) angle, the relative range, and the flight-path angle. They have proved the capturability of the proposed guidance law by studying a Lyapunov-like function. The elliptical arc guidance[8] is another type of the biased PNG for near stationary targets. The main idea of this law is to put the missile on a predetermined elliptical path between the missile and the target. The methods of the second category do not consider the optimization of design parameters such as energy, terminal velocity, and flight time. In general, these guidance laws can require larger control energy than the optimal guidance laws and can generate large guidance commands near the terminal time so as to saturate the command limits.

Because almost all optimal impact angle controllers[1–4,6] are similar in their structure to the linear quadratic optimal guidance law, they can be represented in a unified formulation. In this paper, a generalized formulation of energy minimization optimal guidance laws for constant speed missiles with an arbitrary system order is proposed to achieve the desired impact angle as well as zero miss distance. From the generalized form of the optimal guidance law, we observe that the guidance command is given by a linear combination of the step and the ramp responses of the missile's lateral acceleration. The state feedback optimal guidance laws and their closed-form linear trajectory solutions for the lag-free and the first-order missile dynamics are also derived in this paper.

In the closed-form solutions of optimal control problems, time to go explicitly appears, but it cannot be directly measured from any devices. Hence, to implement the optimal guidance laws, a suitable time to go estimation method is required. Because the time to go of the optimal guidance laws determines guidance gain and control energy, the performance of the optimal guidance laws is critically dependent on the accuracy of time-to-go estimates. Because the trajectory is much curved under the application of the impact angle controllers, the conventional estimation method of time to go from the range over the closing velocity produces large estimation errors, especially in the beginning of the homing phase. In this paper, to overcome this difficulty we propose two kinds of accurate time-to-go calculation methods based on the closed-form optimal trajectory; one is given by the length of curved path over the missile velocity, and the other is the range to go over the mean velocity projected on the line of sight. Both schemes can be used for the proposed optimal guidance laws as well as for other impact angle control methods.

The general formulation of the optimal guidance laws is given in Sec. II. The optimal guidance laws to control the impact angle are then derived, and their closed-form solution are the investigated in

Received 18 February 2004; revision received 3 October 2004; accepted for publication 11 October 2004.

*Ph.D. Candidate, Department of Aerospace Engineering, 373-1 Kusong Yusong; ckryoo@fdcl.kaist.ac.kr. Member AIAA.

†Director, P.O. Box 35-3, Yusung; hjucho@add.re.kr. Member AIAA.

‡Professor, Department of Aerospace Engineering; mjtahk@fdcl.kaist.ac.kr. Member AIAA.

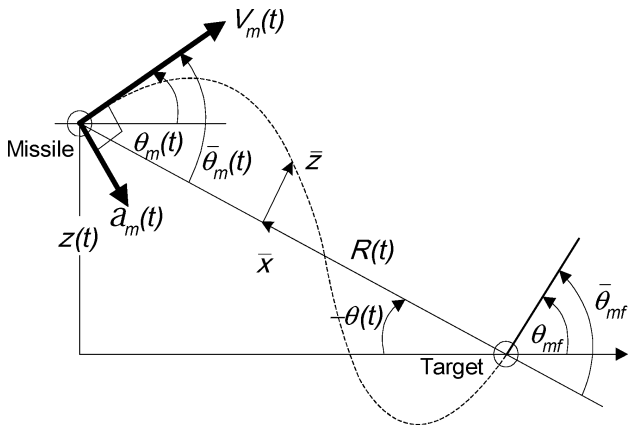

Fig. 1 Homing guidance geometry.

Sec. III. In Sec. IV, two kinds of time-to-go calculation methods are explained. In Sec. V, nonlinear simulation and linear error analysis are conducted to investigate the characteristics of the proposed optimal guidance laws and the time-to-go estimation methods. Finally, the concluding remarks are given in Sec. VI.

II. Generalized Formulation of Optimal Guidance Laws

Consider the homing guidance geometry for a stationary or a slowly moving target shown in Fig. 1. Here, V_m, θ_m, and θ_{mf} denote the missile velocity, the flight-path angle, and the predetermined impact angle, respectively. And a_m is the acceleration applied normal to the velocity vector to change θ_m. Other variables in Fig. 1 are self-explanatory.

The equations of motion for this homing problem are given by

$$\dot{z}(t) = V_m(t)\sin\theta_m(t), \qquad z(0) = 0$$
$$V_m(t)\dot{\theta}_m(t) = -a_m(t), \qquad \theta_m(0) = \theta_{m0} \tag{1}$$

The dynamics of the missile system[9] with a scalar input $u(t)$ is represented by

$$\begin{bmatrix}\dot{a}_m(t)\\ \dot{\boldsymbol{p}}_m(t)\end{bmatrix} = \begin{bmatrix}a_{11} & \boldsymbol{a}_{12}\\ \boldsymbol{a}_{21} & a_{22}\end{bmatrix}\begin{bmatrix}a_m(t)\\ \boldsymbol{p}_m(t)\end{bmatrix} + \begin{bmatrix}b_1\\ \boldsymbol{b}_2\end{bmatrix}u(t)$$
$$\begin{bmatrix}a_m(0)\\ \boldsymbol{p}_m(0)\end{bmatrix} = \begin{bmatrix}0\\ \boldsymbol{0}\end{bmatrix} \tag{2}$$

$$\phi(t_f,t)B = \mathcal{L}^{-1}[sI-A]^{-1}_{t_f-t}B = \mathcal{L}^{-1}\left[\frac{X(s)}{u(s)}\right]_{t_f-t} = \mathcal{L}^{-1}\left[\frac{z(s)}{u(s)} \quad \frac{\theta_m(s)}{u(s)} \quad \frac{a_m(s)}{u(s)} \quad \frac{\boldsymbol{p}_m(s)}{u(s)}\right]^T_{t_f-t}$$
$$= \left[-\mathcal{L}^{-1}\left\{\frac{1}{s^2}\frac{a_m(s)}{u(s)}\right\}_{t_f-t} \quad -\frac{1}{V_m}\mathcal{L}^{-1}\left\{\frac{1}{s}\frac{a_m(s)}{u(s)}\right\}_{t_f-t} \quad \mathcal{L}^{-1}\left\{\frac{a_m(s)}{u(s)}\right\}_{t_f-t} \quad \mathcal{L}^{-1}\left\{\frac{p_m(s)}{u(s)}\right\}_{t_f-t}\right]^T \tag{11}$$

where the missile's acceleration a_m is chosen as the first state variable and $\boldsymbol{p}_m$ is the vector that consists of the remaining $n-1$ state variables. Therefore, a_{11} and b_1 are scalars; $\boldsymbol{a}_{12}$, $\boldsymbol{a}_{21}^T$, and $\boldsymbol{b}_2$ are $(n-1)\times 1$ vectors; and a_{22} is a $(n-1)\times(n-1)$ matrix.

Under the assumption that V_m is constant and θ_m is small, we can linearize Eq. (1) as

$$\dot{z}(t) = V_m\theta_m(t), \qquad \dot{\theta}_m(t) = -a_m(t)/V_m \tag{3}$$

From Eqs. (2) and (3), we obtain the linear differential equation

$$\dot{x} = Ax + Bu, \qquad x(0) = x_0 \tag{4}$$

where

$$x = [z \quad \theta_m \quad a_m \quad \boldsymbol{p}_m]^T \tag{5}$$

$$A = \begin{bmatrix}0 & V_m & 0 & 0\\ 0 & 0 & -1/V_m & 0\\ 0 & 0 & a_{11} & \boldsymbol{a}_{12}\\ 0 & 0 & \boldsymbol{a}_{21} & a_{22}\end{bmatrix}, \qquad B = \begin{bmatrix}0 & 0 & b_1 & \boldsymbol{b}_2^T\end{bmatrix}^T \tag{6}$$

Now, let us consider following optimal control problem: Find $u(t)$, which minimizes J, defined by

$$J = \frac{1}{2}[x(t_f)-x_f]^T S_f[x(t_f)-x_f] + \frac{1}{2}\int_0^{t_f} u^T(\tau)Ru(\tau)\,\mathrm{d}\tau \tag{7}$$

subject to Eq. (4).

Here, $S_f \geq 0$, $R > 0$, whereas t_f and x_f are the time of flight and the desired terminal constraints, respectively.

The solution to this optimal control problem[6] is given by

$$u^* = -R^{-1}B^T\phi^T(t_f,t)S_f[x(t_f)-x_f] \tag{8}$$

where $\phi(t_f,t)$ denotes the state transition matrix to propagate the state from t to t_f, and

$$x(t_f)-x_f = \left[I + \int_t^{t_f}\phi(t_f,\tau)BR^{-1}B^T\phi^T(t_f,\tau)S_f\,\mathrm{d}\tau\right]^{-1}$$
$$\times[\phi(t_f,t)x(t)-x_f] \tag{9}$$

The weighting matrices S_f and R are chosen as

$$S_f = \begin{bmatrix}s_1 & 0 & 0 & 0\\ 0 & V_m s_2 & 0 & 0\\ 0 & 0 & 0 & 0\\ 0 & 0 & 0 & 0\end{bmatrix}, \qquad R = 1 \tag{10}$$

Let $X(s)$ and $u(s)$ be Laplace transform of the state vector $x(t)$ and the scalar input $u(t)$, respectively, then for zero initial conditions we obtain Eq. (11).

Substituting Eqs. (10) and (11) into Eq. (8), an alternative expression of the optimal control input is obtained as

$$u^*(t) = s_1 z(t_f)\mathcal{L}^{-1}\left\{\frac{1}{s^2}\frac{a_m(s)}{u(s)}\right\}_{t_f-t}$$
$$+ s_2[\theta_m(t_f)-\theta_{\mathrm{mf}}]\mathcal{L}^{-1}\left\{\frac{1}{s}\frac{a_m(s)}{u(s)}\right\}_{t_f-t} \tag{12}$$

On the other hand, the term $\phi(t_f, t)x(t) - x_f$ in Eq. (9) implies zero effort miss given by

$$\phi(t_f, t)x(t) - x_f = \mathcal{L}^{-1}[X(s)/x(0)]_{t_f - t}x(t) - x_f \tag{13}$$

where

$$\mathcal{L}^{-1}\left[\frac{X(s)}{x(0)}\right]_{t_f-t} = \mathcal{L}^{-1}\begin{bmatrix} \frac{z(s)}{z(0)} & \frac{z(s)}{\theta_m(0)} & \frac{z(s)}{a_m(0)} & \frac{z(s)}{\boldsymbol{p}_m(0)} \\ \frac{\theta_m(s)}{z(0)} & \frac{\theta_m(s)}{\theta_m(0)} & \frac{\theta_m(s)}{a_m(0)} & \frac{\theta_m(s)}{\boldsymbol{p}_m(0)} \\ \frac{a_m(s)}{z(0)} & \frac{a_m(s)}{\theta_m(0)} & \frac{a_m(s)}{a_m(0)} & \frac{a_m(s)}{\boldsymbol{p}_m(0)} \\ \frac{\boldsymbol{p}_m(s)}{z(0)} & \frac{\boldsymbol{p}_m(s)}{\theta_m(0)} & \frac{\boldsymbol{p}_m(s)}{a_m(0)} & \frac{\boldsymbol{p}_m(s)}{\boldsymbol{p}_m(0)} \end{bmatrix}_{t_f-t} = \begin{bmatrix} 1 & V_m(t_f-t) & -\mathcal{L}^{-1}\left\{\frac{1}{s^2}\frac{a_m(s)}{a_m(0)}\right\}_{t_f-t} & -\mathcal{L}^{-1}\left\{\frac{1}{s^2}\frac{a_m(s)}{\boldsymbol{p}_m(0)}\right\}_{t_f-t} \\ 0 & 1 & -\frac{1}{V_m}\mathcal{L}^{-1}\left\{\frac{1}{s}\frac{a_m(s)}{a_m(0)}\right\}_{t_f-t} & -\frac{1}{V_m}\mathcal{L}^{-1}\left\{\frac{1}{s}\frac{a_m(s)}{\boldsymbol{p}_m(0)}\right\}_{t_f-t} \\ 0 & 0 & \mathcal{L}^{-1}\left\{\frac{a_m(s)}{a_m(0)}\right\}_{t_f-t} & \mathcal{L}^{-1}\left\{\frac{a_m(s)}{\boldsymbol{p}_m(0)}\right\}_{t_f-t} \\ 0 & 0 & \mathcal{L}^{-1}\left\{\frac{\boldsymbol{p}_m(s)}{a_m(0)}\right\}_{t_f-t} & \mathcal{L}^{-1}\left\{\frac{\boldsymbol{p}_m(s)}{\boldsymbol{p}_m(0)}\right\}_{t_f-t} \end{bmatrix}$$

To avoid the inverse of the 4×4 matrix included in Eq. (9), first multiply both sides of Eq. (9) by

$$I + \int \phi(t_f, \tau) B R^{-1} B^T \phi^T(t_f, \tau) S_f \, \mathrm{d}\tau$$

Then, we have two equations related with the terminal states $z(t_f)$ and $\theta_m(t_f) - \theta_{\mathrm{mf}}$ appearing in Eq. (12). After simple calculations, we obtain

$$\begin{aligned} z(t_f) = \frac{1}{\Delta(t)}\Bigg\{ & K_4 z(t) + \Big[K_4 V_m(t_f - t) - K_2\Big]\theta_m(t) + K_2\theta_{\mathrm{mf}} \\ & - \left[K_4\mathcal{L}^{-1}\left\{\frac{1}{s^2}\frac{a_m(s)}{a_m(0)}\right\}_{t_f-t} - \frac{K_2}{V_m}\mathcal{L}^{-1}\left\{\frac{1}{s}\frac{a_m(s)}{a_m(0)}\right\}_{t_f-t}\right]a_m(t) \\ & - \left[K_4\mathcal{L}^{-1}\left\{\frac{1}{s^2}\frac{a_m(s)}{\boldsymbol{p}_m(0)}\right\}_{t_f-t} - \frac{K_2}{V_m}\mathcal{L}^{-1}\left\{\frac{1}{s}\frac{a_m(s)}{\boldsymbol{p}_m(0)}\right\}_{t_f-t}\right]\boldsymbol{p}_m(t)\Bigg\} \end{aligned} \tag{14}$$

$$\begin{aligned} \theta_m(t_f) - \theta_{\mathrm{mf}} & \\ = \frac{1}{\Delta(t)}\Bigg\{ & -K_3 z(t) + \Big[K_1 - K_3 V_m(t_f - t)\Big]\theta_m(t) - K_1\theta_{\mathrm{mf}} \\ & + \left[K_3\mathcal{L}^{-1}\left\{\frac{1}{s^2}\frac{a_m(s)}{a_m(0)}\right\}_{t_f-t} - \frac{K_1}{V_m}\mathcal{L}^{-1}\left\{\frac{1}{s}\frac{a_m(s)}{a_m(0)}\right\}_{t_f-t}\right]a_m(t) \\ & + \left[K_3\mathcal{L}^{-1}\left\{\frac{1}{s^2}\frac{a_m(s)}{\boldsymbol{p}_m(0)}\right\}_{t_f-t} - \frac{K_1}{V_m}\mathcal{L}^{-1}\left\{\frac{1}{s}\frac{a_m(s)}{\boldsymbol{p}_m(0)}\right\}_{t_f-t}\right]\boldsymbol{p}_m(t)\Bigg\} \end{aligned} \tag{15}$$

and

$$\Delta = K_1 K_4 - K_2 K_3$$

$$K_1 = 1 + s_1\int_t^{t_f}\left[\mathcal{L}^{-1}\left\{\frac{1}{s^2}\frac{a_m(s)}{u(s)}\right\}_{t_f-\tau}\right]^2 \mathrm{d}\tau$$

$$K_2 = s_2\int_t^{t_f}\mathcal{L}^{-1}\left\{\frac{1}{s^2}\frac{a_m(s)}{u(s)}\right\}_{t_f-\tau}\mathcal{L}^{-1}\left\{\frac{1}{s}\frac{a_m(s)}{u(s)}\right\}_{t_f-\tau}\mathrm{d}\tau$$

$$K_3 = \frac{s_1}{V_m}\int_t^{t_f}\mathcal{L}^{-1}\left\{\frac{1}{s}\frac{a_m(s)}{u(s)}\right\}_{t_f-\tau}\mathcal{L}^{-1}\left\{\frac{1}{s^2}\frac{a_m(s)}{u(s)}\right\}_{t_f-\tau}\mathrm{d}\tau$$

$$K_4 = 1 + \frac{s_2}{V_m}\int_t^{t_f}\left[\mathcal{L}^{-1}\left\{\frac{1}{s}\frac{a_m(s)}{u(s)}\right\}_{t_f-\tau}\right]^2 \mathrm{d}\tau \tag{16}$$

Equation (12) with Eqs. (14–16) is the general form of optimal guidance law to minimize the impact angle error as well as the miss distance for constant-speed missiles with an arbitrary system order. Although Eqs. (14–16) include time-varying components such as the missile's current states and the time to go, the terminal states $z(t_f)$ and $\theta_m(t_f) - \theta_{\mathrm{mf}}$ are constant for the optimal control u^*. Because the weighting parameters s_1 and $V_m s_2$ in Eq. (10) are also constant, the optimal control u^* given by Eq. (12) is a linear combination of the step response and the ramp response of the missile. For $s_2 = 0$, the resultant optimal guidance law is only concerned with miss distance and equals to the guidance law of Ref. 9.

III. Optimal Guidance Laws for Impact Angle Control

In this section, we derive the closed-form optimal guidance laws for two simple cases and investigate their properties. The first case is a lag-free missile system, and the other is a first-order lag system. Special concerns on the guidance law for the lag-free system are given in this paper because not only does it give us general insights on the higher-order missiles' behavior under the circumstance of impact angle control, but also it can be applied for practical use because of its simplicity. One of the most important properties of the optimal guidance law for the first-order autopilot is more stable near the target for a delayed missile system so that the terminal misses are improved. As it will be explained in Sec. VI, however, the adjoint simulation[10] results show that the miss distance and impact angle error produced by optimal guidance law for perfect autopilot when the first-order autopilot is encountered are negligible if the time of flight is greater than 12 times the time constant.

A. Optimal Guidance Law for Lag-Free Autopilot

Suppose that the missile transfer function is lag free:

$$a_m(s)/u(s) = 1 \tag{17}$$

Then, from Eqs. (12–16), the optimal guidance command is simplified as

$$u^*(t) = s_1 z(t_f) t_{\mathrm{go}} + s_2[\theta_m(t_f) - \theta_{\mathrm{mf}}] \tag{18}$$

where

$$t_{\mathrm{go}} = t_f - t \tag{19}$$

$$z(t_f) = \frac{1}{\Delta(t)}\left[\left(1 + \frac{s_2 t_{\mathrm{go}}}{V_m}\right)z(t) + \left(V_m t_{\mathrm{go}} + \frac{s_2 t_{\mathrm{go}}^2}{2}\right)\theta_m(t) + \frac{s_2 t_{\mathrm{go}}^2}{2}\theta_{\mathrm{mf}}\right] \tag{20}$$

$$\theta_m(t_f) - \theta_{\mathrm{mf}} = \frac{1}{\Delta(t)}\left[-\frac{s_1 t_{\mathrm{go}}^2}{2V_m}z(t) + \left(1 - \frac{s_1 t_{\mathrm{go}}^3}{6}\right)\theta_m(t) - \left(1 + \frac{s_1 t_{\mathrm{go}}^3}{3}\right)\theta_{\mathrm{mf}}\right] \tag{21}$$

$$\Delta = 1 + \frac{s_2 t_{\mathrm{go}}}{V_m} + \frac{s_1 t_{\mathrm{go}}^3}{3} + \frac{s_1 s_2 t_{\mathrm{go}}^4}{12 V_m} \tag{22}$$

Let $s_1 \to \infty$ and $s_2 \to \infty$, then $z(t_f) \to 0$, and $\theta_m(t_f) - \theta_{\mathrm{mf}} \to 0$. Then, we see that

$$u^*(t) = C_R t_{\mathrm{go}} + C_S = \left(V_m / t_{\mathrm{go}}^2\right)[6z(t)/V_m + 4t_{\mathrm{go}}\theta_m(t) + 2t_{\mathrm{go}}\theta_{\mathrm{mf}}] \quad (23)$$

where C_R and C_S are the constant coefficients of the ramp response and the step response given by

$$C_R = s_1 z(t_f) = \left(6V_m / t_{\mathrm{go}}^3\right)[2z(t)/V_m + t_{\mathrm{go}}\theta_m(t) + t_{\mathrm{go}}\theta_{\mathrm{mf}}] \quad (24)$$

$$C_S = s_2[\theta_m(t_f) - \theta_{\mathrm{mf}}] = -\left(2V_m / t_{\mathrm{go}}^2\right)[3z(t)/V_m + t_{\mathrm{go}}\theta_m(t) + 2t_{\mathrm{go}}\theta_{\mathrm{mf}}] \quad (25)$$

For implementing the guidance law given by Eq. (23), the missile only requires a built-in inertial navigation system (INS). If an additional seeker is provided to measure the missile-to-target LOS angle, we can use the LOS angle $-\theta(t)$ instead of $z(t)$. In this case, $\theta(t)$ can be approximated by $-z(t)/V_m t_{\mathrm{go}}$. In this case, Eq. (23) is rewritten as

$$u^*(t) = (V_m/t_{\mathrm{go}})[-6\theta(t) + 4\theta_m(t) + 2\theta_{\mathrm{mf}}] \quad (26)$$

The only obstacle to implement the proposed law given in Eqs. (23) or (26) is how to obtain t_{go}. Accurate and practical calculation methods will be discussed in Sec. IV, where t_{go} is given by the function of $\theta(t)$, $\theta_m(t)$, θ_{mf} and the remaining range.

Integrating Eq. (3) with the boundary conditions

$$z(t_0) = z(t_f) = 0, \qquad \theta_m(t_0) = \theta_{m0}, \qquad \theta_m(t_f) = \theta_{\mathrm{mf}} \quad (27)$$

the closed-form trajectory solutions of $\theta_m(t)$ and $z(t)$ are obtained as

$$\theta_m(t) = (1/V_m)\left(\tfrac{1}{2}C_R t_{\mathrm{go}}^2 + C_S t_{\mathrm{go}} + V_m\theta_{\mathrm{mf}}\right) \quad (28)$$

$$z(t) = -\tfrac{1}{6}C_R t_{\mathrm{go}}^3 - \tfrac{1}{2}C_S t_{\mathrm{go}}^2 - V_m\theta_{\mathrm{mf}} t_{\mathrm{go}} \quad (29)$$

Because the coefficients C_R and C_S are constant, the boundary conditions give

$$C_R = \left(6V_m / t_f^2\right)(\theta_{m0} + \theta_{\mathrm{mf}})$$

$$C_S = (-2V_m/t_f)(\theta_{m0} + 2\theta_{\mathrm{mf}}) \quad (30)$$

This shows that the guidance command profile is dependent on the initial heading angle, the terminal impact angle, and the time of flight. We also note from Eq. (23) that $u^*(t_f)$ is equal to C_S.

It is possible to choose the initial launch angle θ_{m0} for better performance of the guidance law. We have two special initial heading angles; one is to achieve the global minimum energy path, and another is to minimize the magnitude of the guidance command.

In practical points of view, the minimization of control energy is important because it determines the specifications of the actuator system. Let us consider $\bar{J}$ defined as

$$\bar{J} = \int_0^{t_f} u^2(t)\,\mathrm{d}t = \int_0^{t_f} (C_R t_{\mathrm{go}} + C_s)^2\,\mathrm{d}t = \frac{4V_m^2}{t_f}\left(\theta_{m0}^2 + \theta_{m0}\theta_{\mathrm{mf}} + \theta_{\mathrm{mf}}^2\right) \quad (31)$$

Under the assumption that t_f remains constant according to the change of θ_{m0}, then θ_{m0}^*, which minimizes $\bar{J}$, is approximately given by

$$\left[\frac{\partial \bar{J}}{\partial \theta_{m0}}\right]_{\theta_{m0} = \theta_{m0}^*} = 0 \Rightarrow \theta_{m0}^* \simeq -\frac{1}{2}\theta_{\mathrm{mf}} \quad (32)$$

By substituting Eq. (32) into Eqs. (31) and (30), the minimum $\bar{J}$ for the fixed θ_{mf} is obtained as

$$\bar{J}^* \simeq 3V_m^2\theta_{\mathrm{mf}}^2 / t_f \quad (33)$$

and the optimal control history for $\theta_{m0} = \theta_{m0}^*$ is given by

$$u^*(t)|_{\theta_{m0} = \theta_{m0}^*} = -\left(3V_m\theta_{\mathrm{mf}} / t_f^2\right)t \quad (34)$$

Because θ_{m0}^* minimizes $\bar{J}$, $\bar{J}^*$ is the globally minimized cost. In this case, the maximum magnitude of the guidance command occurs at t_f and is given by $|-3V_m\theta_{\mathrm{mf}}/t_f|$.

Severe terminal miss distances and impact angle errors are produced as the guidance command in the terminal phase is saturated. To identify θ_{m0} that guarantees the minimum magnitude of control is also important in two aspects. First, by comparing the minimum magnitude of control with the command limit we can judge whether the saturation occurs or not. Second, by launching the missile with this angle the terminal miss distance caused by command saturation can be avoided.

Because of the linear time-varying property of the command as shown in Eq. (23), the maximum magnitude of the command occurs at $t = 0$ or $t = t_f$.

$$u^{\min} = \min_{\theta_{m0}} \max_t\{|u^*(t)|\} = \min_{\theta_{m0}}\{|u^*(0)|, |u^*(t_f)|\} \quad (35)$$

where

$$u^*(0) = (2V_m/t_f)(2\theta_{m0} + \theta_{\mathrm{mf}}) \quad (36)$$

$$u^*(t_f) = -(2V_m/t_f)(\theta_{m0} + 2\theta_{\mathrm{mf}}) \quad (37)$$

Note that both $u^*(0)$ and $u^*(t_f)$ are represented by two linear functions of θ_{m0} with different slopes. Therefore, the minimum magnitude of guidance command is achieved at the point of intersection of two linear functions, that is, $u^*(0) = u^*(t_f)$. From this condition $\bar{\theta}_{m0}$, the initial heading angle that minimizes the magnitude of the guidance command is obtained as

$$\bar{\theta}_{m0} = -\theta_{\mathrm{mf}} \quad (38)$$

The optimal control with $\theta_{m0} = -\theta_{\mathrm{mf}}$ is then calculated as

$$u^*(t)|_{\theta_{m0} = \bar{\theta}_{m0}} = -2V_m\theta_{\mathrm{mf}}/t_f \quad (39)$$

Note that the optimal control remains constant for all t if the missile is launched with $\bar{\theta}_{m0}$. Because, in this case, the missile flies along a circle as shown in Fig. 2, t_f is simply given by

$$t_f = (R_0/V_m)|\theta_{\mathrm{mf}}/\sin\theta_{\mathrm{mf}}| \quad (40)$$

where R_0 denotes the initial range from the missile to the target.

By substituting Eq. (40) into Eq. (39), we obtain the minimum magnitude of guidance command as

$$u^{\min} \triangleq \left|u^*(t)|_{\theta_{m0} = \bar{\theta}_{m0}}\right| = 2V_m^2|\sin\theta_{\mathrm{mf}}| / R_0 \quad (41)$$

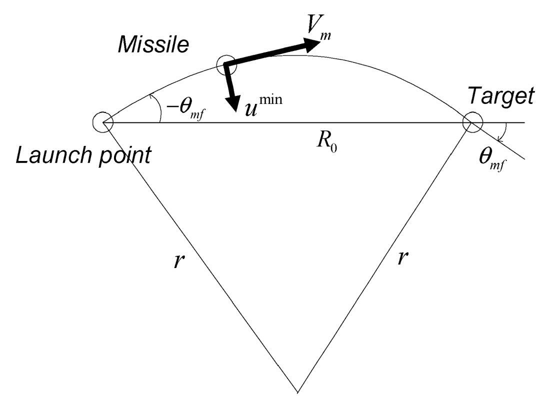

Fig. 2 Circular trajectory by the minimum magnitude of command ($\theta_{m0} = -\theta_{\mathrm{mf}}$).

There is no way to intercept the target with θ_{mf} if the command limit is less than u^{min}. In the case that the command limit is greater than u^{min} but less than $|u^*(0)|$ or $|u^*(t_f)|$, command saturation is inevitably included in the engagement. In this case we can avoid the command saturation by launching the missile with $\theta_{m0} = -\theta_{mf}$. When the command limit is greater than $|-3V_m\theta_{mf}/t_f|$, we can guide the missile along the globally energy minimized trajectory by launching with $\theta_{m0} = -0.5\theta_{mf}$.

B. Optimal Guidance Law for the First-Order Autopilot

Let the missile transfer function be given as a first-order lag system, that is,

$$a_m(s)/u(s) = 1/(\tau s + 1) \tag{42}$$

where τ denotes the time constant. Then, using Eqs. (12–16), the optimal control can be expressed by the state feedback form as

$$\begin{aligned} u^*(t) &= W_1 z(t) + W_2 V_m \theta_m(t) + W_3 V_m \theta_{mf} + W_4 a_m(t) \\ &\approx V_m[-t_{go} W_1 \theta(t) + W_2 \theta_m(t) + W_3 \theta_{mf}] + W_4 a_m(t) \end{aligned} \tag{43}$$

where

$$\begin{aligned} W_1 &= (1/\Delta)(s_1 K_4 D_1 - V_m s_2 K_3 D_2) \\ W_2 &= (1/\Delta)[s_1 D_1 (t_{go} K_4 - K_2) + V_m s_2 D_2 (K_1 - t_{go} K_3)] \\ W_3 &= (1/\Delta)(s_1 K_2 D_1 - V_m s_2 K_1 D_2) \\ W_4 &= (1/\alpha\Delta)[s_1 D_1 (K_2 D_2 - K_4 D_1) + V_m s_2 D_2 (K_3 D_1 - K_1 D_2)] \end{aligned} \tag{44}$$

$$\Delta = K_1 K_4 - K_2 K_3 \tag{45}$$

$$\begin{aligned} K_1 &= 1 + s_1\Big(1/2\alpha^3 + t_{go}\big/\alpha^2 - t_{go}^2\big/\alpha + t_{go}^3\big/3 - 2t_{go}e^{-\alpha t_{go}}\big/\alpha^2 \\ &\quad - e^{-2\alpha t_{go}}\big/2\alpha^3\Big) \\ K_2 &= V_m s_2\Big(1/2\alpha^2 - t_{go}/\alpha + t_{go}^2\big/2 - e^{-\alpha t_{go}}\big/\alpha^2 + t_{go}e^{-\alpha t_{go}}\big/\alpha \\ &\quad + e^{-2\alpha t_{go}}\big/2\alpha^2\Big) \\ K_3 &= s_1 K_2 / V_m s_2 \\ K_4 &= 1 + V_m s_2\Big(t_{go} + 2e^{-\alpha t_{go}}\big/\alpha - 3/2\alpha - e^{-2\alpha t_{go}}\big/2\alpha\Big) \\ D_1 &= t_{go} - 1/\alpha + e^{-\alpha t_{go}}\big/\alpha, \qquad D_2 = (1/V_m)(1 - e^{-\alpha t_{go}}) \\ \alpha &= 1/\tau \end{aligned} \tag{46}$$

As $\tau \to 0$, we can easily show that the optimal control given in Eq. (43) is the same as u^* given in Eq. (18). Note that for the first-order lag system the guidance command goes to zero as $t_{go} \to 0$, while the command for the lag-free system goes to C_S at the terminal time. Because the system's characteristics are not exactly known, the guidance command tends to blow up as the missile approaches the target with some miss distance and impact angle errors. Taking account of the system lag into the guidance law can reduce this instability.

IV. Time-to-Go Calculation Methods

In general, the optimal guidance laws assume that time to go is given. Accurate estimation of time to go is very important because poor estimation of time to go not only severely degrades guidance performance, but also it makes the overall missile trajectory deviate too much from the optimal one.

The most widely used time-to-go calculation method is the range over closing velocity, that is, $t_{go} = R/V_m$. This method gives good estimates of the time to go when PNG-type guidance laws are used on the collision path. For the impact angle control law, however, this method is not adequate because the trajectory for the impact angle control is curved in general. Tahk et al.[11] have suggested a recursive time-to-go computation method, in which the ideal (or minimum) time to go is calculated first and the time-to-go error caused by the path curvature is then compensated. Although this method is originally devised for the optimal guidance laws for varying velocity missiles,[12] it works effectively for various kinds of other guidance laws such as PNG and augmented PNG. In this method, the time-to-go error depends only on the initial heading error. Therefore, the effect of the terminal impact angle constraint on time to go cannot be considered.

In this section, we propose two time-to-go calculation methods adequate for the impact angle control guidance laws. Note that from Eq. (29) the optimal trajectory can be represented by the third-order polynomials of t_{go}. Under the small angle approximation, we have $t_{go} \approx R/V_m$. This implies that the trajectory under the impact angle control laws can be approximated by third-order polynomial functions of the range to go.

As shown in Fig. 1, $\bar{x}$ and $\bar{z}$ are the coordinates of the missile's future trajectory in the LOS frame at t, and $\bar{\theta}_m$ and $\bar{\theta}_{mf}$ are defined as $\bar{\theta}_m = \theta_m + \theta$ and $\bar{\theta}_{mf} = \theta_{mf} + \theta$, respectively. Suppose that $\bar{z}$ is expressed as third-order polynomials of $\bar{x}$;

$$\bar{z}(x) = a_3\bar{x}^3 + a_2\bar{x}^2 + a_1\bar{x} + a_0 \tag{47}$$

From Eq. (3), we have

$$\begin{aligned} \bar{\theta}_m(\bar{x}) &= \dot{\bar{z}}/V_m = \dot{\bar{x}}/V_m\big(3a_3\bar{x}^2 + 2a_2\bar{x} + a_1\big) \\ &\approx -\big(3a_3\bar{x}^2 + 2a_2\bar{x} + a_1\big) \end{aligned} \tag{48}$$

Because Eq. (48) must satisfy the boundary conditions given as

$$\begin{aligned} &\bar{z} = 0, \qquad \bar{\theta}_m = \bar{\theta}_m(t) \qquad \text{and} \qquad \bar{x} = R \quad \text{at} \quad t \\ &\bar{z} = 0, \qquad \bar{\theta}_m = \bar{\theta}_{mf} \qquad \text{and} \qquad \bar{x} = 0 \quad \text{at} \quad t_f \end{aligned}$$

The coefficients of Eqs. (47) and (48) are obtained as

$$\begin{aligned} a_3 &= [-\bar{\theta}_m(t) - \bar{\theta}_{mf}]\big/R^2, \qquad a_2 = [2\bar{\theta}_m(t) + \bar{\theta}_{mf}]/R \\ a_1 &= -\bar{\theta}_{mf}, \qquad a_0 = 0 \end{aligned} \tag{49}$$

Now time to go can be calculated in two ways; one is the length of the curved path over the velocity V_m (method 1), and the other is the range R over the average velocity $\bar{V}_m$, which is the projection of the velocity vector on the LOS (method 2). The detailed expression of these two methods is shown in Table 1. The major difference between the two methods lies in the binomial series approximation of the second-order term of the integrand. The approximations included in Table 1 are valid only for $-1 < (z')^2 < 1$ in method 1, while for $-\infty < \bar{\theta}_m < \infty$ in method 2. However, $(z')^2 \geq 1$ necessarily occurs as θ_{m0} and θ_{mf} are closer to $\pi/2$. For large θ_{m0} and θ_{mf}, method 1 produces larger time-to-go calculation error than method 1. The proposed time-to-go calculation methods are independent of guidance laws, and they can be applied to other kinds of impact angle controllers.

V. Simulation Results

In this section, the performance of the optimal guidance law for lag-free autopilot is studied. First, nonlinear simulations for the proposed law for the lag-free system on various situations are performed to investigate the basic properties. Second, error analyses using the adjoint technique[10] for the first-order lag missile system are performed. Third, the proposed optimal guidance law is compared with other impact angle control law. Fourth, the capture conditions on the initial heading angle and the terminal impact angle are investigated under the existence of the command limits. Finally, the technique to alleviate the performance degradation as a result of the command limits is tested.

Table 1 Comparisons of time-to-go calculation methods

Method	Equations	Approximation
1 Length of the curved path over velocity	$t_{go} = \dfrac{1}{V_m}\displaystyle\int_0^R \sqrt{1+(z')^2}\,dx$, where $z' = \dfrac{dz}{dx}$	$\sqrt{1+(z')^2}$
	$\approx \dfrac{R}{V_m}\left[1 + \dfrac{\bar\theta_m^2 + \bar\theta_{mf}^2}{15} - \dfrac{\bar\theta_m\bar\theta_{mf}}{30} - \dfrac{\bar\theta_m^4 + \bar\theta_{mf}^4}{140}\right.$	$\approx 1 + \dfrac{1}{2}(z')^2 - \dfrac{1}{8}(z')^4$
	$\left. + \dfrac{\bar\theta_m\bar\theta_{mf}\left(\bar\theta_m^2 + \bar\theta_{mf}^2 - \bar\theta_m\bar\theta_{mf}\right)}{280}\right]$	$= 1 + \dfrac{1}{2}\theta_m^2 - \dfrac{1}{8}\theta_m^4$
2 Range over average velocity	$t_{go} = \dfrac{R}{\bar V_m}$	
	$\bar V_m = \dfrac{1}{R}\displaystyle\int_0^R V_m\cos\bar\theta_m\,dx \approx V_m\left[1 - \dfrac{\bar\theta_m^2 + \bar\theta_{mf}^2}{15} + \dfrac{\bar\theta_m\bar\theta_{mf}}{30}\right.$	$\cos\bar\theta_m \approx 1 - \dfrac{\bar\theta_m^2}{2!} + \dfrac{\bar\theta_m^4}{4!}$
	$\left. + \dfrac{\bar\theta_m^4 + \bar\theta_{mf}^4}{420} - \dfrac{\bar\theta_m\bar\theta_{mf}\left(\bar\theta_m^2 + \bar\theta_{mf}^2 - \bar\theta_m\bar\theta_{mf}\right)}{840}\right]$	

Table 2 Initial conditions for nonlinear simulations

Parameter	Value
Missile position x_{m0}, z_{m0}	0 m, 0 m
Missile velocity V_m	200 m/s
Target position x_{t0}, z_{t0}	0 m, 5000 m
Initial heading angle θ_{m0}	90 deg
Impact angle θ_{mf}	-90 deg $\le \theta_{mf} \le 90$ deg every 30 deg

Table 3 Comparisons of the time-to-go calculation methods for the lag-free autopilot ($\theta_{m0} = 90$ deg)

	$\Delta t_{f_{max}}/t_f$, %			J, m²/s³		
θ_{mf}, deg	R/V_m	Method 1	Method 2	R/V_m	Method 1	Method 2
−90	−31.9	−17.6	−0.4	54,922	51,770	50,207
−60	−23.3	−9.6	0.6	47,129	45,010	44,320
−30	−16.9	−5.4	0.8	48,788	47,279	46,889
0	−31.2	−3.7	0.8	64,516	63,213	62,906
30	−12.6	−3.4	0.7	95,043	93,361	93,023
60	−15.3	−4.4	0.5	136,720	133,576	132,931
90	−21.3	−8.1	−0.1	182,831	176,244	174,318

A. Comparisons of Time-to-Go Calculation Methods

For the initial conditions shown in Table 2, the optimal guidance law given in Eq. (26) is considered. We assume that the missile has perfect measurements on θ_m, V_m, and θ, and there are no command limits. Table 3 shows the comparison results for three kinds of the time-to-go calculation methods: $t_{go} = R/V_m$, method 1, and method 2 described in Table 1. The index $\Delta t_{f_{max}}/t_f$ denotes the normalized maximum estimation error of t_f, where

$$\Delta t_{f_{max}} = \max_{0 \le t \le t_f} \left\{ t_f^*(t) - t_f \right\}$$

and $t_f^*(t) = t_{go} + t$. From this table, we find that R/V_m gives very poor estimates of time to go, whereas method 1 is quite accurate and method 2 is the best, as expected (see Sec. IV). The time histories of the estimated t_{go} for the sample cases are shown in Figs. 3 and 4, where we observe that method 1 and R/V_m tend to underestimate time to go. This is mainly because the length of the path to be divided by the velocity is smaller than the true one. Table 3 shows that the control energy is required less as the time to go is more accurate.

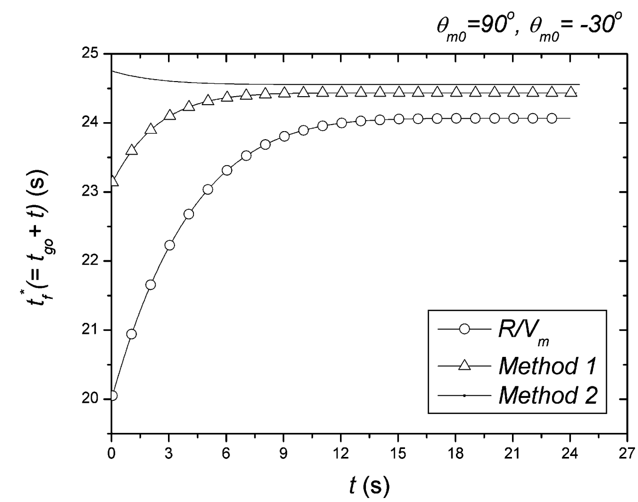

Fig. 3 Comparison of the estimates of the time of flight for θ_{m0} = 90 deg, $\theta_{mf} = -30$ deg.

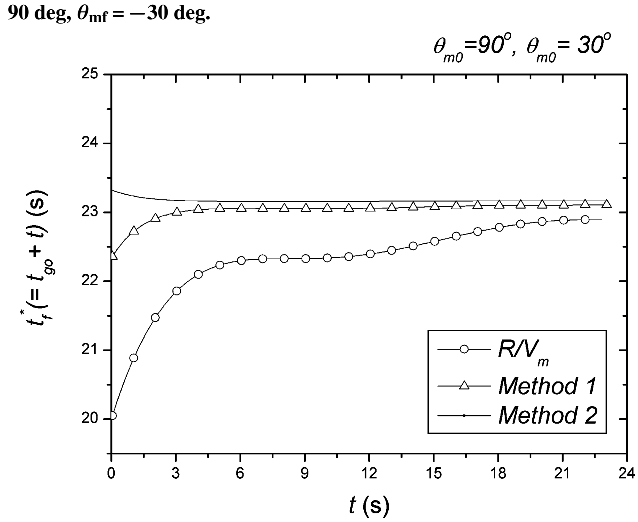

Fig. 4 Comparison of the estimates of the time of flight for θ_{m0} = 90 deg, $\theta_{mf} = 30$ deg.

B. Investigation of Basic Properties

Missile trajectories obtained by using method 2 for various θ_{mf} with $\theta_{m0} = 90$ deg are shown in Fig. 5. The ramp and step coefficients C_R and C_S should be constant in the ideal cases. However, as shown in Figs. 6 and 7, C_R and C_S are not constant if the impact angle is too large for the linear approximation of the equations of motion to be useful. Thus, the guidance command is not perfectly linear to t_{go} for high impact angles, as shown in Fig. 8, although the time-to-go estimates of method 2 are still quite accurate. In these nonlinear simulations, discussions on the terminal errors in distances and impact angles are meaningless because we assume no uncertainties in the system.

Figure 9 shows the trajectories for very high launch and impact angle. Although the capture region is varied from the initial launch conditions and the range, lots of simulations show that the proposed

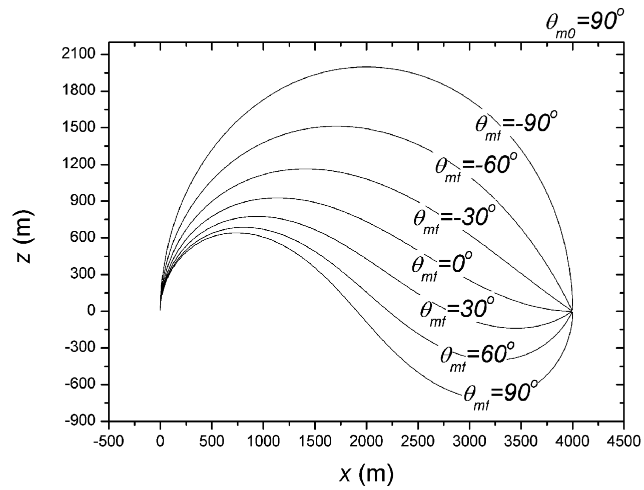

Fig. 5 Energy optimal trajectories for various impact angles.

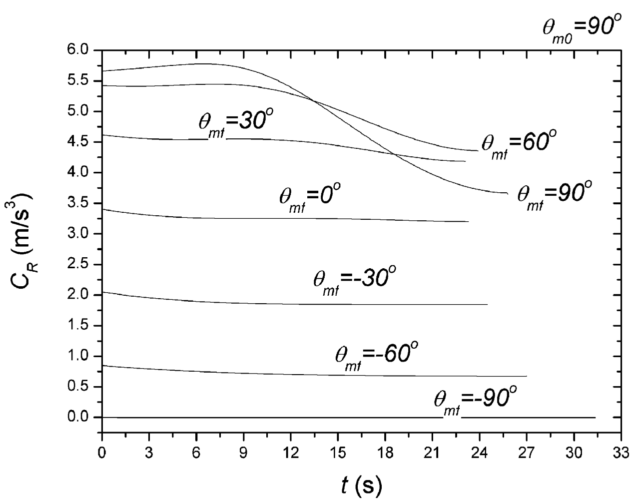

Fig. 6 Histories of the coefficient of ramp response.

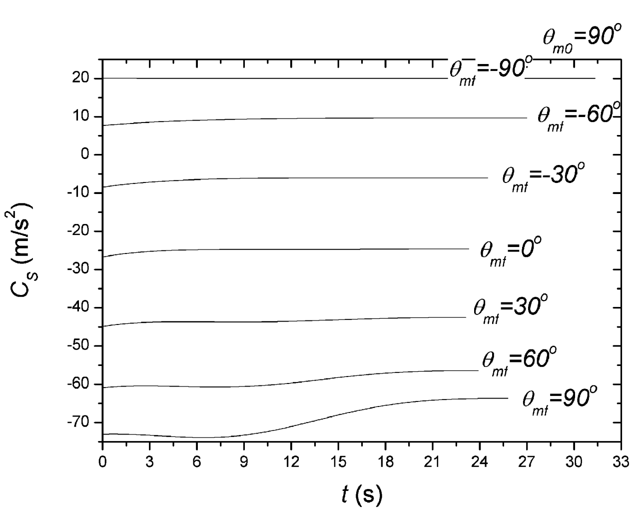

Fig. 7 Histories of the coefficient of step response.

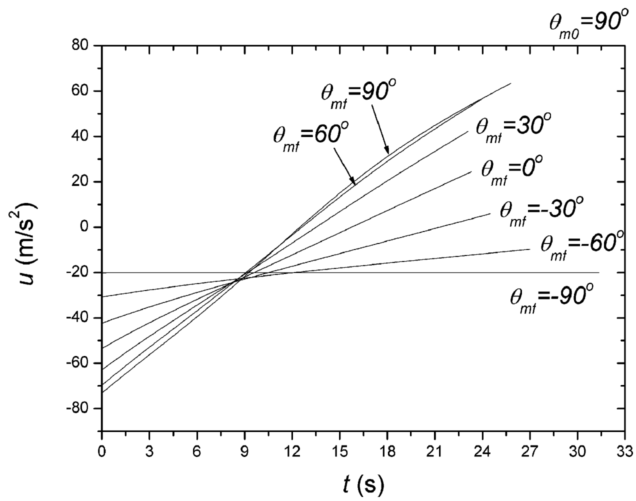

Fig. 8 Resultant guidance command histories.

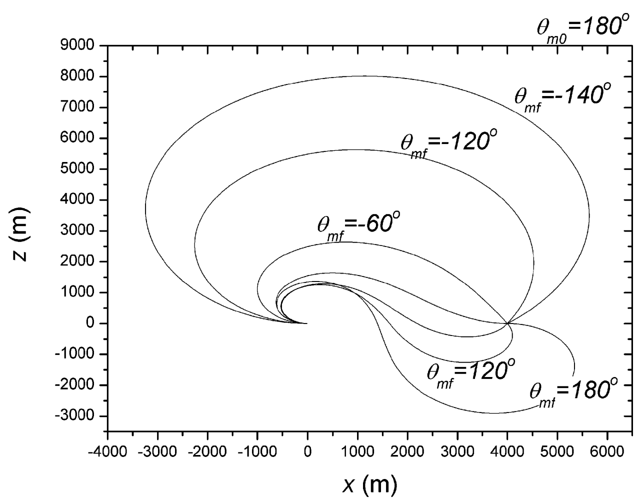

Fig. 9 Trajectories for high launch and impact angles.

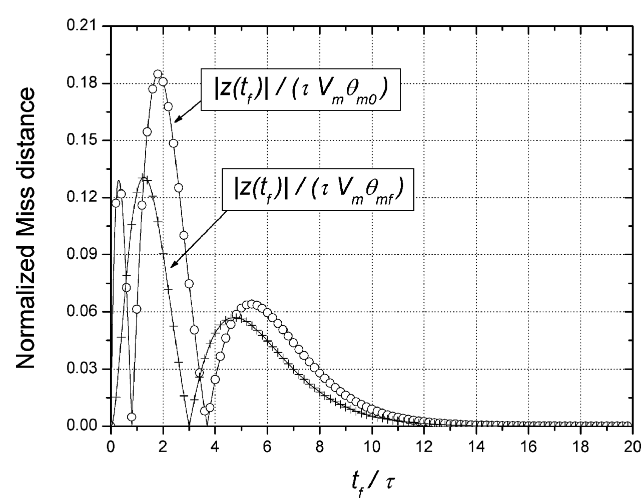

Fig. 10 Normalized miss distances induced by θ_{m0} and θ_{mf}.

law has large capture region. For the initial position of the missile shown in Table 1, the capture region is approximately given by $-140\ \mathrm{deg} \leq \theta_{\mathrm{mf}} \leq 180\ \mathrm{deg}$ for $\theta_{m0} = 180$ deg.

C. Adjoint Simulations

Now let us consider the terminal errors as a result of the system lag. Figures 10 and 11 show the results of the linear error analysis using the adjoint simulation technique, where the first-order lag autopilot given by Eq. (42) is assumed while the guidance command is produced by the optimal guidance law for the lag-free system as given in Eq. (23). It is observed that both miss distance and impact angle error are significantly affected by the initial heading angle. Therefore, one can effectively reduce the terminal errors by control of the initial heading errors. The terminal miss is negligible if t_f is more than 12 times the time constant τ. This implies that the missile must be launched far from the target to guarantee a small terminal miss. Figure 10 shows that for small t_f very large impact angle errors are induced as a result of abrupt increase in the guidance command.

Table 4 Comparisons of OGL with BPN for the lag-free autopilot ($\theta_{m0} = 60$ deg)

	OGL (t_{go}-method 2)		BPN ($N = 4.0$, $\eta = 1.3$)	
θ_{mf}, deg	t_f, s	J, $\mathrm{m^2/s^3}$	t_f, s	J, $\mathrm{m^2/s^3}$
−60	24.2	29,015	25.2	30,957
−30	22.3	23,100	22.5	23,132
0	21.5	31,665	21.6	33,630
30	21.5	55,980	21.3	66,101
60	22.4	92,187	21.7	111,933
90	24.2	132,203	23.3	147,500

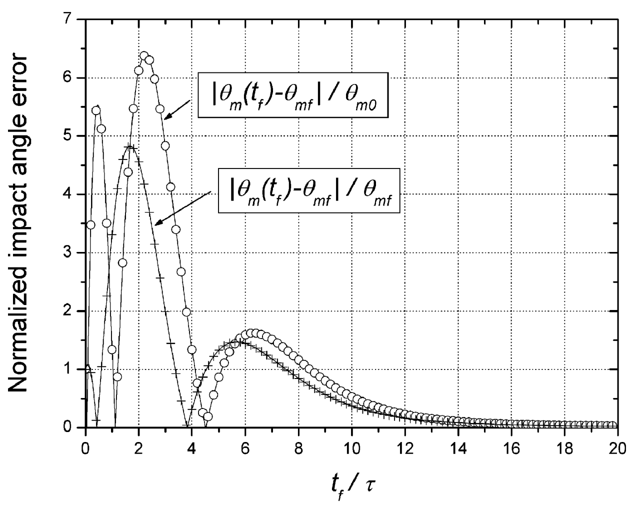

Fig. 11 Normalized impact angle errors induced by θ_{m0} and θ_{mf}.

Because this is not fit in reality, the trend of impact angle errors in the adjoint simulations is just concerned.

D. Comparisons with Other Impact Angle Control Law

The performance of the proposed optimal guidance law (OGL) is compared with biased proportional navigation (BPN) described in Ref. 7, which can be expressed as

$$u_{\mathrm{BPN}}(t) = N V_m[\dot{\theta}(t) - \dot{\theta}_b(t)] \tag{50}$$

where N is a navigation constant, $\dot{\theta}(t)$ is the LOS rate, and $\dot{\theta}_b$ denotes the time-varying biased term to control the impact angle defined by

$$\dot{\theta}_b(t) = \frac{\eta V_m[\theta_d - \theta(t)]}{N R(t)\cos[\theta_m(t) - \theta(t)]} \tag{51}$$

Here, η is an arbitrary positive constant, and θ_d is the desired LOS angle at the time of impact, which can be replaced by θ_{mf}. It is noted that from Eq. (51) that BPN is singular when $\theta_m(t) - \theta(t)$ so that the capture region and launch envelope of BPN are limited more than OGL. The most attractive feature of BPN is that it does not include time to go.

To avoid the singularity, simulations are done for $\theta_{m0} = 60$ deg and $\theta_{\mathrm{mf}} = -60$ deg ∼ 90 deg. Other initial conditions are given in Table 2. We choose $N = 4.0$ and $\eta = 1.3$ for BPN according to Ref. 7. The time-to-go calculation method 2 is used for OGL. From Table 4, OGL spends less control energy than BPN. Figures 12 and 13 show the comparison results of trajectories and guidance command histories for several θ_{m0} and θ_{mf}, respectively. From Fig. 13, we observe that the command of BPN tends to blow up as the missile approaches the target. This implies that large terminal miss distances and impact angle errors for BPN can be produced if the command limit is active.

E. Error Analysis for Command Saturation

The other major error source is the command limit. Because the optimal guidance command for the lag-free system is represented by θ_{m0}, θ_{mf}, and t_f as given in Eqs. (23) and (30), the launch envelope

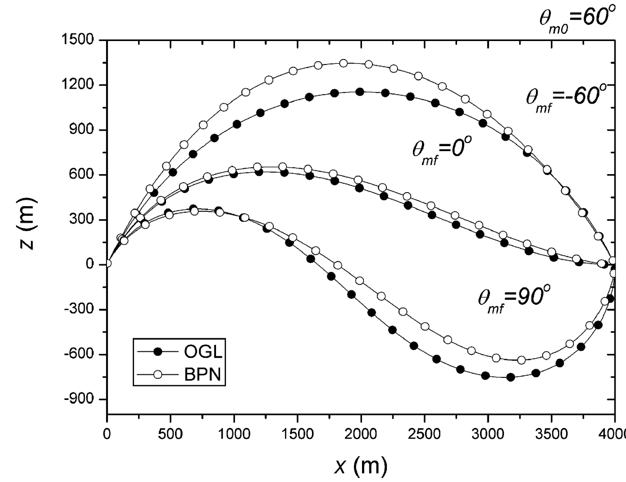

Fig. 12 Trajectories of OGL and BPN.

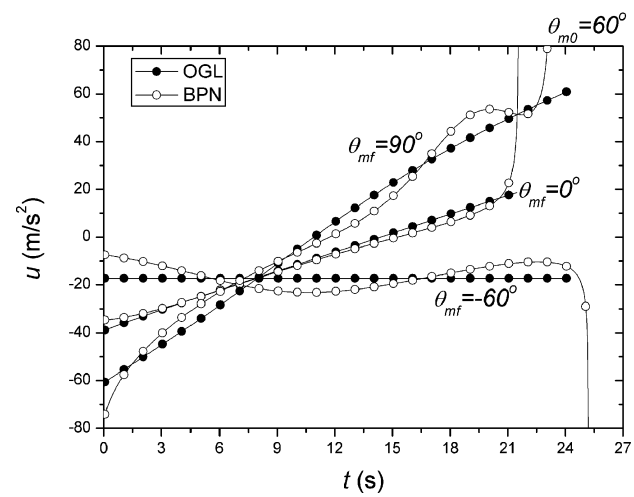

Fig. 13 Guidance command histories of OGL and BPN.

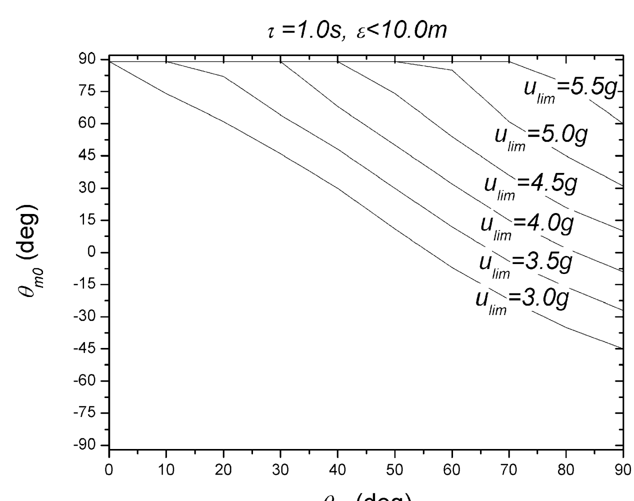

Fig. 14 Envelope of θ_{m0} vs θ_{mf} for permissible error.

of θ_{m0} vs θ_{mf} can be specified for a given τ and the initial positions of the missile and the target. Figure 14 provides the launch envelope of θ_{m0} vs θ_{mf} for various command limits u_{lim}, where the terminal errors are included in the admissible error bound defined by

$$\varepsilon \triangleq \sqrt{R^2(t_f) + \{V_m[\theta_m(t_f) - \theta_{\mathrm{mf}}]\}^2} \le 10\ \mathrm{m} \tag{52}$$

In this simulation, the initial conditions of Table 2 and $\tau = 1$ s are assumed. It is observed from Fig. 13 that the launch envelope becomes gradually smaller as $u_{\lim}$ decreases. If the current launch conditions are out of the envelope, one might have to change θ_{m0} or make the missile follow a predetermined trajectory in the initial flight phase, in order to avoid large terminal error caused by the command saturation.

VI. Conclusions

In this paper, we have proposed the generalized form of the energy minimization optimal guidance laws represented as a linear combination of the step and the ramp acceleration responses of the missile. Based on this work frame, the optimal impact angle-control guidance laws for the lag free and the first-order autopilot are proposed.

The proposed guidance laws not only give the energy optimality but also have the wide launch-impact angle envelope and the bounded control throughout the engagement. The command histories of the proposed laws can be easily predicted and changed by the choice of a proper initial heading angle to avoid or alleviate the difficulties typically met in the real world such as system lag and command saturation. The performance of the optimal guidance laws is critically dependent on the accuracy of time-to-go estimates. We propose new practical time-to-go calculation methods based on the fact that missile's trajectory can be effectively approximated by a third-order polynomial function of the range to go. The time-to-go calculation method 2, range over averaged velocity along the line of sight, shows good accuracy within 1% error as verified by nonlinear simulations for high initial heading angles and impact angles. A built-in INS is enough to implement the proposed optimal guidance laws and the time-to-go calculation methods because the current position (or line-of-sight angle) and the velocity of the missile are only required.

References

[1]Kim, M., and Grider, K. V., "Terminal Guidance for Impact Attitude Angle Constrained Flight Trajectories," *IEEE Transactions on Aerospace and Electronic Systems*, Vol. AES-9, No. 6, 1973, pp. 852–859.

[2]Bryson, A. E., Jr., and Ho, Y.-C., *Applied Optimal Control*, Wiley, New York, 1975, pp. 154, 155.

[3]Ryoo, C. K., and Cho, H., "Optimal Guidance with Terminal Impact Angle and Control Constraint," *Proceedings of the 1992 Korean Automatic Control Conference*, Korean Automatic Control Council, Seoul, Republic of Korea, 1992, pp. 601–606 (in Korean).

[4]Ben-Asher, J. Z., and Yaesh, I., *Advances in Missile Guidance Theory*, Progress in Astronautics and Aeronautics, Vol. 180, AIAA, Reston, VA, 1998, pp. 25–32.

[5]Song, T. L., and Shin, S. J., "Time-Optimal Impact Angle Control for Vertical Plane Engagements," *IEEE Transactions on Aerospace and Electronic Systems*, Vol. 35, No. 2, 1999, pp. 738–742.

[6]Song, T. L., Shin, S. J., and Cho, H., "Impact Angle Control for Planar Engage Engagements," *IEEE Transactions on Aerospace and Electronic Systems*, Vol. 35, No. 4, 1999, pp. 1439–1444.

[7]Kim, B. S., Lee, J. G., and Han, H. S., "Biased PNG Law for Impact with Angular Constraint," *IEEE Transactions on Aerospace and Electronic Systems*, Vol. 34, No. 1, 1998, pp. 277–288.

[8]Felio, D. A., and Duggan, D. S. (Instructors), "Lecture Note on Autonomous Vehicle Guidance, Control, and Simulation," 2000 Aerospace Short Course of the Univ. of Kansas Continuing Education, San Diego, CA, Sept. 2000.

[9]Rusnak, I., and Meir, L., "Modern Guidance Law for High-Order Autopilot," *Journal of Guidance, Control, and Dynamics*, Vol. 14, No. 5, 1991, pp. 1056–1058.

[10]Zarchan, P., *Tactical and Strategic Missile Guidance*, 2nd ed., Progress in Astronautics and Aeronautics, Vol. 157, AIAA, Washington, DC, 1994, pp. 49–58.

[11]Tahk, M. J., Ryoo, C. K., and Cho, H., "Recursive Time-to-Go Estimation for Homing Guidance Missiles," *IEEE Transactions on Aerospace and Electronic Systems*, Vol. 38, No. 1, 2002, pp. 13–24.

[12]Cho, H., Ryoo, C. K., and Tahk, M. J., "Implementation of Optimal Guidance Laws Using Predicted Velocity Profiles," *Journal of Guidance, Control, and Dynamics*, Vol. 22, No. 4, 1999, pp. 579–588.